Volume 1 | Number 1 | Jan 2013 | Pages 1–100

PCCP

Physical Chemistry Chemical Physics
www.rsc.org/pccp

ROYAL SOCIETY OF CHEMISTRY

This is an *Accepted Manuscript*, which has been through the Royal Society of Chemistry peer review process and has been accepted for publication.

Accepted Manuscripts are published online shortly after acceptance, before technical editing, formatting and proof reading. Using this free service, authors can make their results available to the community, in citable form, before we publish the edited article. We will replace this *Accepted Manuscript* with the edited and formatted *Advance Article* as soon as it is available.

You can find more information about *Accepted Manuscripts* in the **Information for Authors**.

Please note that technical editing may introduce minor changes to the text and/or graphics, which may alter content. The journal's standard **Terms & Conditions** and the **Ethical guidelines** still apply. In no event shall the Royal Society of Chemistry be held responsible for any errors or omissions in this *Accepted Manuscript* or any consequences arising from the use of any information it contains.

Journal Name

Dynamic Article Links ▶

ARTICLE TYPE

Fullerene Assemblies toward Photo-energy Conversions

Yanfei Shen[a] and Takashi Nakanishi[b]*

5 Manipulating molecular interaction and assembly for developing various functional nanostructures with controlled dimensionality, morphology and tailored properties are currently a research focus in molecular science and materials chemistry. Particularly, the self-organization of fullerenes (i.e. C_{60}) to form various functional assemblies has received intense interest since it can provide excellent optoelectronic properties for photo-energy conversion-induced applications such as solar cells and field effect transistors (FET).
10 In this perspective, we describe our recent efforts on the development in the area of fullerene molecular design and assemblies aimed at improving the photoconductivity and photo-energy (electric and thermal) conversion systems.

1. Introduction

The unique spherical structure of fullerenes, with sp^2-hybridized
15 carbon atoms and extended π-conjugation, produces numerous fascinating optoelectronic properties, which have gathered much interest for applications in nanoelectronics and photovoltaics.[1, 2] In particular, C_{60} was found to behave as a strongly electron-accepting molecule able to reversibly accept up to six electrons.
20 In addition, C_{60}, C_{70} and their derivatives show exceptional electronic absorption bands expanding throughout the entire UV-Vis spectrum, which is promising an extensive use in photovoltaic devices such as solar cells and FET.[3-5] Therefore, manipulating the intermolecular interaction and assembly of
25 fullerenes in nano/micrometer length scale is crucial for developing various functional nanostructures with controlled dimensionality and tailored properties. However, precise fine-tuning the π-π interaction in adjacent spherical-shaped pristine fullerenes is still challenging although the face-to-face packing of
30 planar conjugated-π units is rather well known.[1, 6] As a result, various C_{60} derivatives themselves or with electron-donating organic/inorganic compounds have been designed and studied towards constructing highly functional, sophisticated assembled materials and improving performance in organic-based
35 optoelectronic devices,[2, 7-11] and are still a challenging task.[12]

The recent interest of fullerene research in materials chemistry is mainly devoted to the understanding of molecular-level interaction and morphology-oriented functions and applications.[1, 6] Because of the high potential in fullerene-
40 containing materials for photovoltaic development, our most recent achievements of the advanced controlling assembly of C_{60} and its derivatives towards improved photoconductivity and applications used photo-energy, i.e. electric and thermal, conversion processes will be presented. The alkyloxyphenyl
45 substituted *N*-methylfulleropyrrolidine, namely, alkylated-C_{60}[13] (Scheme 1), as a new family of C_{60} derivatives, has received considerable attention in recent years. They have shown a variety

of interesting properties and functions in the development of soft materials such as liquid crystals, solvent-free liquids and other
50 assembled architectures with various shapes and dimensions for the areas of photo-energy conversions.
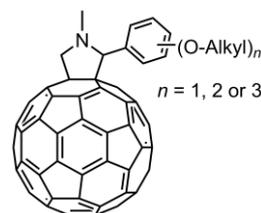
Scheme 1. Schematic illustration of a typical structural example of alkylated-C_{60} derivatives, where "Alkyl" represents linear or branched
55 long alkyl chains.

2. Fullerene Assemblies with Enhanced Photoconductivity

2.1 Alkylated Fullerene Assemblies

The intrinsic properties of C_{60} are expected to be transferred or
60 modulated in the film and/or bulk materials by forming various self-assembled C_{60} architectures. For instance, a high performance solution-processed thin-film transistor (TFT) based on an alkylated-C_{60} was successfully fabricated.[14] Liquid crystals (LCs) are a state of matter between the liquid and the solid state,
65 which are referred to as intermediate phases or mesophases. C_{60} is one kind of promising electron-transporting materials as an n-type organic semiconductor due to its spherical π-conjugated framework that can easily accept and transport electron through the ordered structure.[15, 16] Recently, C_{60}-based LCs have been
70 found applications in photovoltaics because of the optoelectronic features as well as the self-organization ability at molecular level in a pre-determined and controllable fashion, also with their softness in developing flexible devices.[17-19] However, the content of C_{60} is usually low due to the attached large and bulky
75 mesogens for the effective alignment of C_{60} units, which may be

one of the main factors for the low carrier mobility. Our group recently reported that the alkylated-C_{60} derivatives such as **1** (Figure 1a) with high C_{60} content (up to 50% in case of only two linear chains attachment) satisfy the requirements for high carrier mobility in the mesophase.[20] As revealed by differential scanning calorimetry (DSC) and polarized optical microscopic (POM) studies, **1** shows a mesophase the wide temperature range between 62 and 193 °C (Figure 1b), proved by its fluid and birefringent characteristics. The attached alkyl chains adjust the π-π interactions between C_{60} units to form a regularly ordered lamellar (smectic) phase. Further detailed organized structure has been investigated, an alternative arrangement of the C_{60} units and the molten alkyl chains with an interlayer distance of 5.59 nm, by combination analysis of X-ray diffraction (XRD) and electron density profile simulation (Figure 1c,d).[21] It should be mentioned that the electrochemical and optoelectronic properties of **1** are maintained in the mesomorphic state. For instance, the mesomorphic state of **1** exhibits reversible redox activity as cast films on a glassy carbon electrode. The electron mobility was found to be ~3×10^{-3} cm^2 V^{-1} s^{-1} from a time-of-flight (TOF) measurement, indicating that dense packed C_{60} molecules carried charges efficiently. This mobility value is comparable to those of smectic LCs of organic semiconductor oligomers and columnar LCs.[22, 23] The simple modification of C_{60} by long alkyl chains permits a high C_{60} content in the mesomorphic materials, resulting in the large electron mobility value for C_{60}-containing LCs reported.
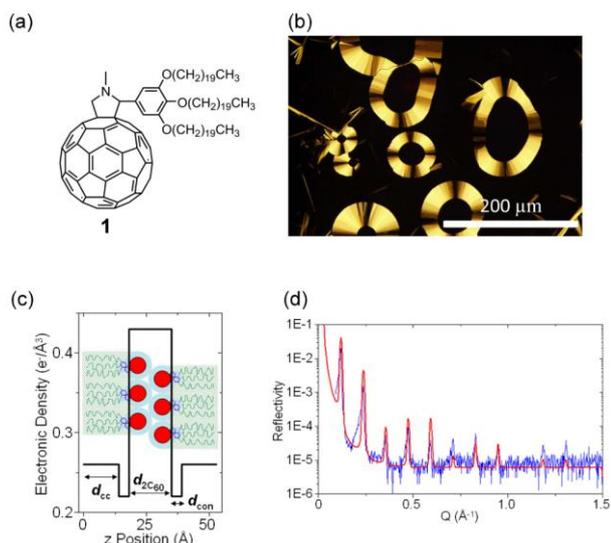

Figure 1. (a) Chemical structure of **1**; (b) polarizing optical microscope texture of lamellar mesophase of **1** at 190 °C.[20] Reproduced with permission from ref. 20. Copyright 2008 American Chemical Society; (c) three-box electronic density profile and (d) comparison between the corresponding model (red line) and the experimental XRD pattern (blue line) of **1** in the mesophase.[21] Reproduced with permission from ref. 21. Copyright 2010 American Chemical Society.

A dedicate balance of the intermolecular interactions introduced by C_{60}-C_{60} and van der Waals forces among the attached units, and the assembly environments leads to a wide variety of supramolecular architectures and functions, which provides an effective way for sophisticated molecular design of C_{60} derivative.[7, 13] For instance, attachment of branched aliphatic

chains on π-conjugated molecule can soften π-based materials and enables the formation of thermotropic LCs and room temperature nonvolatile liquids.[24-26] As we reported recently, the alkylated-C_{60} bearing two swallow tail-type alkyl chains at the (3,5)-positions of the phenyl moiety (**2**, Figure 2a) has a melting point of only 84 °C, which is approximately 109 °C lower than that of **1**, and exhibits a smectic phase extending to room temperature (Figure 2b).[24] The bulk heterojunction organic solar cells composed of an active layer of **2** and poly(3-hexylthiophene) (P3HT) shows a power conversion efficiency (PCE) of 1.6%, which is comparable to that of [6,6]-phenyl-C61-butyric acid methyl ester (PCBM)/P3HT in our device setup. On the contrary, the composite of **1** and P3HT exhibits a PCE of only 0.5% under the same experimental condition (Figure 2c). The improvement of open-circuit voltage (V_{OC}) for **2**/P3HT compared with those of PCBM/P3HT and **1**/P3HT could be caused by the difference of their interfacial interaction with P3HT.[27, 28] The improved performance of **2**/P3HT system could be ascribed to the presence of the branched aliphatic chains, which may facilitate lowering the crystallinity and improving the charge transport capability. This makes such molecules good candidates for the preparation of organic solar cells with soft and flexible characteristics.
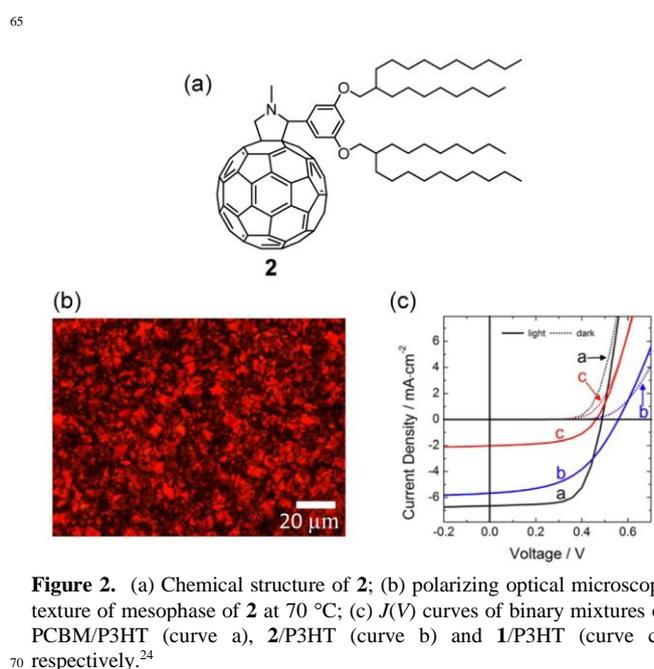

Figure 2. (a) Chemical structure of **2**; (b) polarizing optical microscope texture of mesophase of **2** at 70 °C; (c) $J(V)$ curves of binary mixtures of PCBM/P3HT (curve a), **2**/P3HT (curve b) and **1**/P3HT (curve c), respectively.[24]

2.2 Fullerene Coassemblies

High C_{60} content and appropriate π stacking orientation in the semiconducting active layer in photovoltaic devices is significantly important to retain better performance. In this context, basically insulating alkyl chains commit negative influence in reduction of C_{60} content. Generally smaller substituent groups are attached on C_{60} towards improvement of their optoelectronic properties.[29, 30] What happens if there are no alkyl chain attachments in the same phenyl substituted *N*-methylfulleropyrrolidines? Solvent vapor diffusion is a unique strategy for the preparation of crystalline materials from solution. By using this method, the coassembly of C_{60} derivatives has been

used to develop millimeter-sized flat crystalline sheets with ordered surface pattern and morphology.[31] As shown in Figure 3, the phenyl and perfluorophenyl interaction[32] in the small substitution units has been used to control the solubility and assembly properties of C_{60} derivatives **3** and **4** (Figure 3a).[31] Atomic force microscope (AFM) images (Figure 3b) of the crystal surface show long straight patterns which exhibits the presence of well-ordered steps with an average height of ~2.0 nm, while the single crystal X-ray analysis revealed the bimolecular layer organization of the molecules throughout the crystal. The coassembled crystal exhibits good anisotropy, with over double the charge carrier mobility in the parallel direction to the plane of the crystal than perpendicular to the plane due to the dense π-stacking along the surface of the crystal (Figure 3c). The development of such large flat sheet crystals with anisotropies will be useful in different switchable optoelectronic devices.
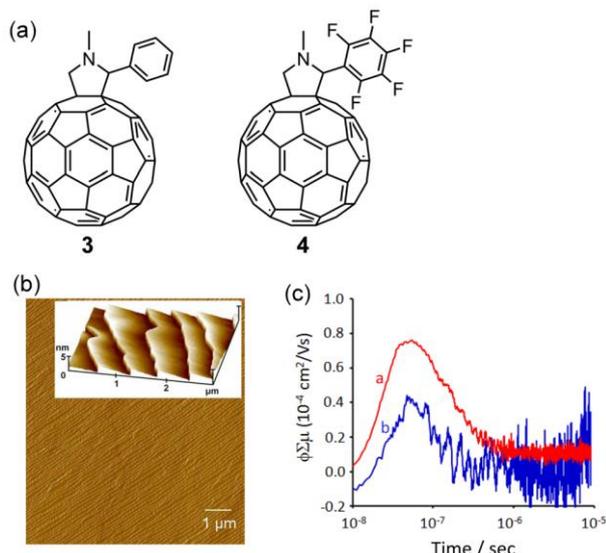

Figure 3. (a) Chemical structures of **3** and **4**; (b) AFM images of the coassembly of **3** and **4**; (c) TRMC transient decay profiles in the parallel (curve a) and perpendicular (curve b) directions.[31]

Constructing composites of inorganic nanocrystals (NCs) and organic molecules are attractive for the economical optoelectronic applications in the concept of flexible devices.[33, 34] Recently, solvent-free, photoconductive or emissive organic liquid materials have been developed as a new type of organic soft materials.[35] Their unique features such as nonvolatility, tunable optic and/or electronic functions, solvent-free processing, and the ability to act as solvent/matrix for other organic or inorganic components, are essential for their practical applications. In this context, various solvent-free liquid materials and composites have been reported by our group.[26, 36] For example, the nanocomposite of cadmium selenide (CdSe) nanocrystals (NCs) embedded in photoconductive liquid C_{60} derivative **5**[37] (Figure 4a) has been prepared.[38] The CdSe NCs are well-dispersed in the liquid phase of **5**, as confirmed by HR-TEM analysis of a 1:1 (by weight) blending of **5** and CdSe NCs. The steady-state photoluminescence (PL) measurements show that the PL from optically excited CdSe NCs is dramatically quenched in 10 wt% of **5**, which can be ascribed to the favorable van der Waals interaction between the hexadecylamine ligands on

CdSe NCs and alkyl pendant groups of **5**. The photoelectrochemical measurements of the solvent-free CdSe NCs/**5** composite film on FTO electrode show that the photocurrent under white light illumination is 2 fold and under blue-light illumination is 3 fold higher than those of pure CdSe NCs (Figure 4b). The LUMO level difference of CdSe NCs (−3.84 eV) and C_{60} (−4.30 eV) facilitates exciton separation of photo-generated excitons in the CdSe NCs phase as well as electron transfers from CdSe NCs to **5**, which was supported by the cathodic photocurrents in the photoelectrochemical measurements in Figure 4b.[38] This result shows that the inter-phase charge transfer in CdSe NCs/**5** composites provides a convenient route for conversion of optical energy to electrical energy.
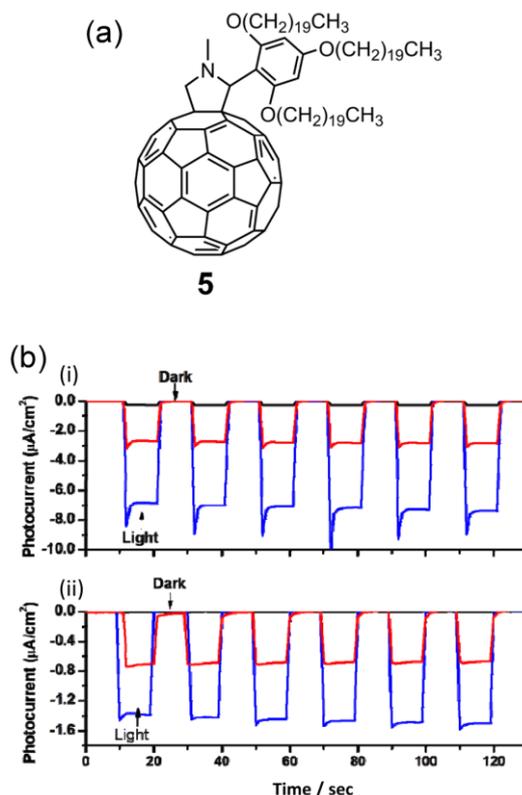

Figure 4. (a) Chemical structure of **5**; (b) photoelectrochemical activity of solvent-free CdSe NC/**5** composite films on FTO-coated glass containing 0 wt% (black), 25 wt% (blue) and 100 wt% CdSe NC (red) under (i) white light illumination and (ii) blue light (at 480 nm) illumination.[38]

3. Photo-energy Conversion in Nanocarbon Hybrids

Nanocarbon hybrids have received intense interest towards developing lightweight and flexible devices. The hybridization of C_{60} with single-wall carbon nanotubes (SWCNT) would couple the optical and electronic properties of SWCNT together with the electron-accepting feature of C_{60}.[39-46] The high affinity of the alkylated-C_{60} towards the graphitic structure[8] allows direct assembly between alkylated-C_{60} and SWCNT surface followed by the formation of microstructure composites.[47] When sonicated in a solvent such as THF, a stable dispersion of **1**/SWCNT can be

obtained. The direct interaction between **1** and SWCNT facilitated charge transport and charge collection. The photoinduced electron transfer was proven by the combination of several spectroscopic techniques such as steady-state and time-resolved fluorescence studies, and the nanosecond transient absorption. For instance, the nanosecond transient absorption studies show the presence of the C_{60} radical anion upon laser illumination for **1**/SWCNT, however, it is not observed for **1**, indicating that **1** acts as an acceptor (Figure 5a). The photoelectrochemical measurements revealed a prompt, steady and reproducible short-circuit photocurrent of the hybrid, which is about 160 fold larger than that of **1**, and 18 fold larger than that of SWCNT (Figure 5b). Photoconductivity evaluations by using a single-SWCNT field-effect transistor (FET) device showed that the decoration of SWCNT by **1** in the nanodevice has induced a transition of gate transfer characteristics (Figure 5c). The **1**-decorated SWCNT-FET shows unipolar p-type transport with gate threshold voltage positively shifting by ~5 V, while the SWCNT-FET shows ambipolar characteristics. This p-type characteristic is attributed to the charge transfer between **1** and local parts of SWCNT, suggesting that **1** exerts a strong electron acceptor effect on SWCNT. With a similar way, the decoration of graphene devices with clusters of **1** (Figure 5d) shows clear hole-doping effects and a pronounced increase in gate hysteresis upon illumination with visible light, enabling the use of the C_{60}-graphene hybrid materials in three-terminal photo-memory devices.[48]
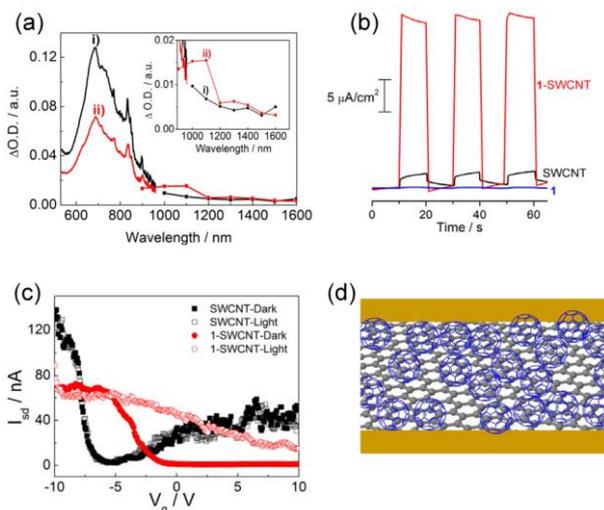

Figure 5. (a) Nanosecond transient absorption spectra of **1** (curve i) and **1**-SWCNT (curve ii) in THF using 355 nm laser irradiation. Inset: enlarged absorption curve (900-1600 nm); (b) short-circuit photocurrent response of **1**/FTO (blue line), SWCNT/FTO (black line) and **1**-SWCNT/FTO (red line) under white light (150 W Xe lamp); (c) evolution of the gate transfer (I_{sd}-V_g) characteristics of **1**-decorated SWCNT-nano FET with and without light illumination, bias voltages V_{sd} = 100 mV;[47] (d) schematic illustration of the **1**/graphene hybrid device.[48] Reproduced with permission from Ref. 48.

The photo-thermal conversion feature of SWCNT upon absorbing near-infrared (NIR) light has the potential for a wide range of applications such as drug delivery and cancer therapies.[49-51] Although the local temperature change is crucial for the applications, the accurate measurement of temperature increase induced by the SWCNT local heating is challenging.[52] In this regard, the microparticles or microplates containing C_{60} derivatives (i.e., **1**) and SWCNT have been developed as a temperature indicator,[39] where SWCNT is used as a light antenna and **1** as a matrix (Figure 6). The temperature rises upon NIR irradiation was confirmed via the melt-induced morphological change of nanocarbons assemblies. Due to the noncovalent interaction between **1** and the side walls of SWCNT, minute amount of SWCNTs can be debundled in 1,4-dioxane at 70 ˚C with sonication. Upon cooling to room temperature, a uniform coassembly of **1** and SWCNT was obtained, whose morphology and microparticle structure (Figure 6) are similar with those of only **1**,[9] as revealed by SEM, HR-cryo-TEM, FTIR, and XRD studies. Upon NIR laser illumination, the flake-shaped **1**-SWCNT assemblies started to "deform" and melt. In contrast, the microparticles only composed of **1** did not response to the laser illumination, suggesting that the heating is due to the "photo-thermal conversion" of SWCNT. The deformation of the micrometer-scale C_{60}-SWCNT assembly can easily be visualized by optical microscopy, thus providing great convenience in monitoring temperature in situ during photo-thermal conversion. Moreover, the assembly melting point can be tuned to a desired range by the molecular design of C_{60} derivative. Thus, C_{60}-SWCNT coassembly can be used as a temperature indicator for the photothermal conversion of SWCNT under NIR light irradiation. By incorporating gold nanoparticles or SWCNT into the C_{60} assemblies, the coassemblies were used for the precise control of the surface architecture on the micrometer length scale, i.e., to initiate particle fusion, partial melting of the aggregates, and bridging particles.[53] Moreover, the surface wetting control can also be achieved via this technique. Our current research concept can be adopted for many applications such as local wetting control, lithography and morphological control of the functional materials.[53]
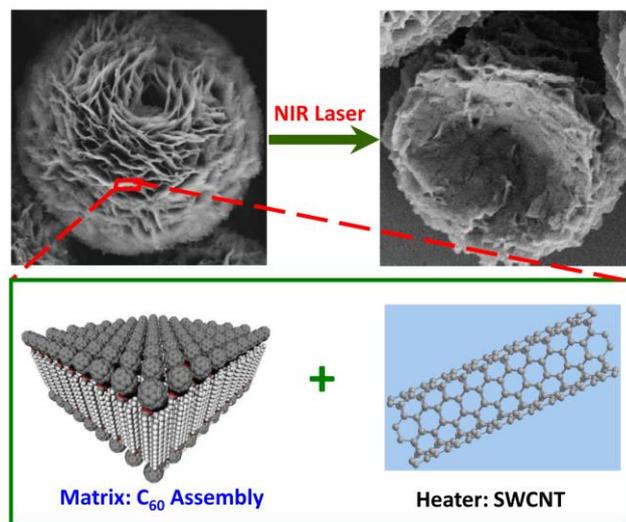

Figure 6. Scheme of the **1**-SWCNT assembly for evaluating photo-thermal conversion of SWCNT.[39] Reproduced with permission from ref. 39. Copyright 2010 American Chemical Society.

4. Conclusion and Outlook

Functionalizing C_{60} by attaching a variety of alkyl chains facilitates fine-tuning the intermolecular interaction, and herein

the functional assemblies and materialization. By precisely controlling the C_{60}-C_{60} interaction, assembled nanostructures and surface morphology, C_{60} based soft materials exhibit promising properties and specific optoelectronic functions. The coassemblies of alkylated-C_{60} with sophisticated organic/inorganic compounds with specific tasks such as designing suitable D/A systems were proved to be an effective way for enhanced photoconductivity and photovoltaic performance. In other cases, the hybridization of alkylated-C_{60} with SWCNT allows constructing temperature indicator for the photo-thermal conversion of SWCNT upon NIR light irradiation. It is therefore clear that alkylated-C_{60} for the self-assembly and assembly control of molecular constructs by assembling different binding motifs offers opportunities for the development of new generation, nanocarbon-based soft materials towards applications in photo-energy conversion. These advanced fullerene assemblies are opening up bright avenues for the chemist in the exploitation of new properties and applications. It should be emphasized that now these researches are surely directing for further soft materializations and development of devices equipped them, and our effort would be beneficial in those future endeavor.

Acknowledgements

Notes and references

a Medical School, Southeast University, Nanjing, 210009, China;
b National Institute for Materials Science (NIMS), 1-2-1 Sengen, Tsukuba, 305-0047, Japan

E-mail: NAKANISHI.Takashi@nims.go.jp

1. S. S. Babu, H. Möhwald and T. Nakanishi, *Chem. Soc. Rev.*, 2010, **39**, 4021.
2. A. Montellano Lopez, A. Mateo-Alonso and M. Prato, *J. Mater. Chem.*, 2011, **21**, 1305.
3. D. M. Guldi, B. M. Illescas, C. M. Atienza, M. Wielopolskia and N. Martín, *Chem. Soc. Rev.*, 2009, **38**, 1587.
4. D. M. Guldi, N. Martín and M. Prato, *J. Mater. Chem.*, 2008, **18**, 1415.
5. K. M. Kadish and R. S. Ruoff, *Electrochemistry of Fullerenes*, Wiley Interscience, New York, 2000.
6. H. Li, J. Choi and T. Nakanishi, *Langmuir*, 2013, **29**, 5394.
7. T. Nakanishi, Y. Shen, J. Wang, H. Li, P. Fernandes, K. Yoshida, S. Yagai, M. Takeuchi, K. Ariga, D. G. Kurth and H. Möhwald, *J. Mater. Chem.*, 2010, **20**, 1253.
8. T. Nakanishi, N. Miyashita, T. Michinobu, Y. Wakayama, T. Tsuruoka, K. Ariga and D. Kurth, *J. Am. Chem. Soc.*, 2006, **128**, 6328.
9. T. Nakanishi, T. Michinobu, K. Yoshida, N. Shirahata, K. Ariga, H. Möhwald and D. G. Kurth, *Adv. Mater.*, 2008, **20**, 443.
10. J. L. Delgado, P. de la Cruz, A. Urbina, J. T. L. Navarrete, J. Casado and F. Langa, *Carbon*, 2007, **45**, 2250.
11. S. Giordani, J.-F. Colomer, F. Cattaruzza, J. Alfonsi, M. Meneghetti, M. Prato and D. Bonifazi, *Carbon*, 2009, **47**, 578.
12. P. Innocenzi and G. Brusatin, *Chem. Mater.*, 2001, **13**, 3126.
13. T. Nakanishi, *Chem. Commun.*, 2010, **46**, 3425.
14. Y. Horii, K. Sakaguchi, M. Chikamatsu, R. Azumi, K. Yase, M. Kitagawa and H. Konishi, *Appl. Phys. Express*, 2010, **3**, 101601.
15. N. S. Sariciftci, D. Braun, C. Zhang, V. I. Srdanov, A. J. Heeger, G. Stucky and F. Wudl, *Appl. Phys. Lett.*, 1993, **62**, 585.
16. M. Morana, M. Wegscheider, A. Bonanni, N. Kopidakis, S. Shaheen, M. Scharber, Z. Zhu, D. Waller, R. Gaudiana and C. Brabec, *Adv. Funct. Mater.*, 2008, **18**, 1757.
17. C.-Z. Li, Y. Matsuo and E. Nakamura, *J. Am. Chem. Soc.*, 2009, **131**, 17058.
18. W. S. Li, Y. Yamamoto, T. Fukushima, A. Saeki, S. Seki, S. Tagawa, H. Masunaga, S. Sasaki, M. Takata and T. Aida, *J. Am. Chem. Soc.*, 2008, **130**, 8886.
19. D. Guillon, B. Donnio and R. Deschenaux, *Liquid-Crystalline Fullerodendrimers and Fullero(Codendrimers)*, in *Fullerene Polymers: Synthesis, Properties and Applications*, eds. N. Martin and F. Giacalone, Wiley-VCH, Weinheim, 2009, pp. 247.
20. T. Nakanishi, Y. Shen, J. Wang, S. Yagai, M. Funahashi, T. Kato, P. Fernandes, H. Möhwald and D. G. Kurth, *J. Am. Chem. Soc.*, 2008, **130**, 9236.
21. P. A. L. Fernandes, S. Yagai, H. Möhwald and T. Nakanishi, *Langmuir*, 2009, **26**, 4339.
22. M. Funahashi and J. I. Hanna, *Adv. Mater.*, 2005, **17**, 594.
23. S. M. Tuladhar, D. Poplavskyy, S. A. Choulis, J. R. Durrant, D. D. C. Bradley and J. Nelson, *Adv. Funct. Mater.*, 2005, **15**, 1171.
24. H. Li, S. S. Babu, S. T. Turner, D. Neher, M. J. Hollamby, T. Seki, S. Yagai, Y. Deguchi, H. Möhwald and T. Nakanishi, *J. Mater. Chem. C*, 2013, **1**, 1943.
25. M. J. Hollamby and T. Nakanishi, *J. Mater. Chem. C*, 2013, **1**, 6178.
26. S. S. Babu, J. Aimi, H. Ozawa, N. Shirahata, A. Saeki, S. Seki, A. Ajayaghosh, H. Möhwald and T. Nakanishi, *Angew. Chem. Int. Ed.*, 2012, **51**, 3391.
27. P. P. Khlyabich, B. Burkhart and B. C. Thompson, *J. Am. Chem. Soc.*, 2011, **133**, 14534.
28. R. A. Street, D. Davies, P. P. Khlyabich, B. Burkhart and B. C. Thompson, *J. Am. Chem. Soc.*, 2013, **135**, 986.
29. C.-C. Chu, G. Raffy, D. Ray, A. D. Guerzo, B. Kauffmann, G. Wantz, L. Hirsch and D. M. Bassani, *J. Am. Chem. Soc.*, 2010, **132**, 12717.
30. X. Zhang, T. Nakanishi, T. Ogawa, A. Saeki, S. Seki, Y. Shen, Y. Yamauchi and M. Takeuchi, *Chem. Commun.*, 2010, **46**, 8752.
31. S. S. Babu, A. Saeki, S. Seki, H. Möhwald and T. Nakanishi, *Phys. Chem. Chem. Phys.*, 2011, **13**, 4830.
32. K. Reichenbacher, H. I. Suss and J. Hulliger, *Chem. Soc. Rev.*, 2005, **34**, 22.
33. J. H. Bang and P. V. Kamat, *ACS Nano*, 2011, **5**, 9421.
34. D. M. Guldi, I. Zilbermann, G. Anderson, N. A. Kotov, N. Tagmatarchis and M. Prato, *J. Am. Chem. Soc.*, 2004, **126**, 14340.
35. S. S. Babu and T. Nakanishi, *Chem. Commun.*, 2013, **49**, 9373.
36. S. S. Babu, M. J. Hollamby, J. Aimi, H. Ozawa, A. Saeki, S. Seki, K. Kobayashi, K. Hagiwara, M. Yoshizawa, H. Möhwald and T. Nakanishi, *Nat. Commun.*, 2013, **4**, 1969.
37. T. Michinobu, T. Nakanishi, J. Hill, M. Funahashi and K. Ariga, *J. Am. Chem. Soc.*, 2006, **128**, 10384.
38. T. J. Kramer, S. S. Babu, A. Saeki, S. Seki, J. Aimi and T. Nakanishi, *J. Mater. Chem.*, 2012, **22**, 22370.
39. Y. Shen, A. G. Skirtach, T. Seki, S. Yagai, H. Li, H. Möhwald and T. Nakanishi, *J. Am. Chem. Soc.*, 2010, **132**, 8566.
40. F. D'Souza, R. Chitta, A. S. D. Sandanayaka, N. K. Subbaiyan, L. D'Souza, Y. Araki and O. Ito, *J. Am. Chem. Soc.*, 2007, **129**, 15865.
41. D. M. Guldi, E. Menna, M. Maggini, M. Marcaccio, D. Paolucci, F. Paolucci, S. Campidelli, M. Prato, G. M. Aminur Rahman and S. Schergna, *Chem. Eur. J.*, 2006, **12**, 3975.
42. T. Umeyama, N. Tezuka, M. Fujita, S. Hayashi, N. Kadota, Y. Matano and H. Imahori, *Chem. Eur. J.*, 2008, **14**, 4875.
43. J. K. J. van Duren, X. Yang, J. Loos, C. W. T. Bulle-Lieuwma, A. B. Sieval, J. C. Hummelen and R. A. J. Janssen, *Adv. Funct. Mater.*, 2004, **14**, 425.
44. Y. Yamamoto, G. Zhang, W. Jin, T. Fukushima, N. Ishii, A. Saeki, S. Seki, S. Tagawa, T. Minari, K. Tsukagoshi and T. Aida, *Proc. Natl. Acad. Sci. USA*, 2009, **106**, 21051.

45. M. S. Arnold, J. D. Zimmerman, C. K. Renshaw, X. Xu, R. R. Lunt, C. M. Austin and S. R. Forrest, *Nano Lett.*, 2009, **9**, 3354.
46. T. Tajima, W. Sakata, T. Wada, A. Tsutsui, S. Nishimoto, M. Miyake and Y. Takaguchi, *Adv. Mater.*, 2011, **23**, 5750.
47. Y. Shen, J. S. Reparaz, M. R. Wagner, A. Hoffmann, C. Thomsen, J.-O. Lee, S. Heeg, B. Hatting, S. Reich, A. Saeki, S. Seki, K. Yoshida, S. S. Babu, H. Mohwald and T. Nakanishi, *Chem. Sci.*, 2011, **2**, 2243.
48. E. K. Jeon, C. S. Yang, Y. F. Shen, T. Nakanishi, D. S. Jeong, J. J. Kim, K. S. Ahn, K. J. Kong and J. O. Lee, *Nanotechnology*, 2012, **23**, 455202.
49. N. W. S. Kam, M. O'Connell, J. A. Wisdom and H. Dai, *Proc. Natl. Acad. Sci. USA*, 2005, **102**, 11600.
50. S. Ghosh, S. Dutta, E. Gomes, D. Carroll, R. Agostino, J. Olson, M. Guthold and W. H. Gmeiner, *ACS Nano*, 2009, **3**, 2667.
51. E. Miyako, K. Kono, E. Yuba, C. Hosokawa, H. Nagai and Y. Hagihara, *Nat. Commun.*, 2012, **3**, 1226.
52. E. Miyako, H. Nagata, K. Hirano and T. Hirotsu, *Angew. Chem. Int. Ed.*, 2008, **47**, 3610.
53. H. Asanuma, P. Subedi, J. Hartmann, Y. Shen, H. Möhwald, T. Nakanishi and A. Skirtach, *Langmuir*, 2013, **29**, 7464.

Table of Contents

Fullerene Assemblies toward Photo-energy Conversions

5

Yanfei Shen and Takashi Nakanishi*
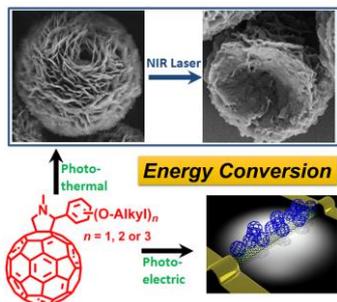
10 Manipulating the molecular interaction and assembly of fullerene derivatives leads to enhanced photoconductivity and applications in photo-energy (electric and thermal) conversion systems.